

## First-Principles Phonon and Multiple-Scattering Electron-Energy-Loss-Spectra Studies of Cu(111) and Ag(111)

Y. Chen and S. Y. Tong

*Laboratory for Surface Studies and Department of Physics, University of Wisconsin-Milwaukee, Milwaukee, Wisconsin 53201*

K. P. Bohnen and T. Rodach

*Kernforschungszentrum Karlsruhe G.m.b.H., Institut für Nukleare Festkörperphysik, Postfach 3640, Karlsruhe, Germany*

K. M. Ho

*Ames Laboratory and Department of Physics, Iowa State University, Ames, Iowa 50011*

(Received 19 November 1992)

Parameter-free first-principles phonon calculations are used in conjunction with multiple-scattering electron-energy-loss calculations to reveal new localized modes on Cu(111) and Ag(111). The discovery of these  $z$ -polarized localized modes along  $\bar{\Gamma}\bar{M}$  and  $\bar{\Gamma}\bar{K}$  provides for the first time good agreement between theory and all the existing helium-atom-scattering and electron-energy-loss experimental results. The new results indicate that it is not necessary to evoke exotic models such as anomalous surface dynamical effects on these densely packed surfaces.

PACS numbers: 61.14.Hg, 63.20.Dj

Over the past decade, inelastic He atom scattering (HAS) and high-resolution electron-energy-loss spectroscopy (EELS) have contributed substantially to our understanding of surface phonon modes for a wide variety of clean and adsorbate-covered metal and semiconductor surfaces. The availability of accurate measurements from the two techniques and the complementary nature of such data have contributed significantly to the resolution of some long-standing issues of surface lattice dynamics. However, despite promising progress, there still exists major difficulties in the interpretation of recent HAS and EELS data even on some simple surfaces.

The noble and transition metal surfaces, Ag(111) and Cu(111), are the best known examples [1-8]. It was known from structural studies that they underwent very small geometric relaxations [9,10]; therefore no large force constant modifications could be expected on these densely packed surfaces. This simple physical picture, however, seemed to be in strong disagreement with observations based on HAS measurements. The difficulty arose from the fact that HAS measurements revealed two surface modes along high symmetry directions  $\bar{\Gamma}\bar{M}$  and  $\bar{\Gamma}\bar{K}$ . Theoretical results based on simple force constant models have long predicted also two surface modes along these directions: a low-lying  $z$ -polarized (i.e., normal to the surface) Rayleigh mode  $S_1$  and a longitudinal mode. The disagreement occurs for the predicted frequencies of the longitudinal mode, which were substantially higher than those of the second mode measured by HAS [1,2]. To explain this discrepancy, novel surface dynamical models were proposed which softened the intralayer surface force constants by 48% in Ag(111) [3] and 67% in Cu(111) [11]. It was proposed that the HAS data were evidence that anomalous surface dynamical effects existed in Ag(111) and Cu(111). Major attempts were made

to explain the dramatic softening, e.g., in terms of charge redistribution at the surface [5], weakening of  $sp-d$  hybridization [4], and changes in coordination for the surface atoms [6].

When EELS data for Cu(111) [7] became available, analysis of the data by Hall *et al.* [7] led to a major clarification of the modes. The longitudinal mode ( $S_2$ ) along  $\bar{\Gamma}\bar{M}$  was measured and its frequency lay in the phonon band gap near  $\bar{M}$  [7]. Clearly this mode cannot be the second mode observed by HAS. The measured frequency of this mode could be well fitted by a simple force constant model with a small (15%) softening of the intralayer surface force constant. This raised some serious questions on the large-softening force constant models. A semiempirical embedded-atom-model (EAM) study explained the second mode observed by HAS along  $\bar{\Gamma}\bar{M}$  in terms of a dispersion crossing avoidance of first- and second-layer sagittal modes [8]. In this interpretation, the second mode along  $\bar{\Gamma}\bar{M}$  has a surface-layer-dominated longitudinal character in the first half of the zone. In the second half of the zone, this mode switched to having a second-layer  $z$  character. However, this assignment could not fit well the measured second mode dispersion. This problem is particularly serious for Ag(111), where it is again necessary to apply a large ( $\sim 50\%$ ) surface force softening to bring the calculated frequency in agreement with that of the HAS measurement.

In this paper, we suggest a completely different interpretation based on a parameter-free first-principles total-energy and phonon calculation [12]. Along  $\bar{\Gamma}\bar{M}$ , our results revealed two first-layer-dominated  $z$ -polarization structures; they are the Rayleigh mode  $S_1$  and a  $z$ -polarized resonance which we call  $R_1$ . These two features explain the observations of He scattering which are primarily sensitive to the  $z$ -direction charge fluctuation.

A third localized structure, longitudinal in its first-layer polarization, is the  $S_2$  mode whose frequency falls in the band gap near  $\bar{M}$ . This mode was measured by EELS for Cu(111) [7]. We show that the presence of these three localized structures is demonstrated by analyzing the energy dependence of the EELS cross section. Using different incident electron energies and scattering geometries, we seek out conditions in which either the Rayleigh mode  $S_1$ , the longitudinal mode  $S_2$ , or the z-polarized resonance  $R_1$ , dominate over the EELS spectra. A series of comparisons between theory and experiment for the EELS cross sections are presented to isolate the effects of the three localized structures. There is no longer a need for evoking an anomalously large surface force-constant softening in either Cu(111) or Ag(111) and our results for the first time provide a consistent explanation of all existing HAS and EELS data.

The theoretical model is based on the first-principles calculation using a norm-conserving pseudopotential [13] and the interpolated form of the Hedin-Lundqvist formula [14] for the electronic exchange and correlation. In addition to the total energy, the forces exerted on each atomic layer are calculated using the Hellmann-Feynman theorem [15]. We first determine the equilibrium posi-

TABLE I. Comparison of calculated and measured (from Ref. [2]) frequencies (in THz) of the  $S_1$  mode at  $\bar{M}$  and  $\bar{K}$ .

		Calculation	Experiment
Cu(111)	$\bar{M}$	3.3	3.2
	$\bar{K}$	3.4	3.4
Ag(111)	$\bar{M}$	2.2	2.1
	$\bar{K}$	2.1	2.2

tions of the surface atoms. The calculated relaxations are indeed very small [16], in excellent agreement with the experimental results. The calculated surface charge densities are shown in Fig. 1. It is apparent from the figure that the surface charge density is very bulklike, except for regions well outside the first layer of atoms. This picture is consistent with what we expect for a densely packed surface. Based on these structural and electronic properties, a large softening in the *intralayer* surface force constants is very unlikely.

To calculate the phonon spectra at high symmetry points  $\bar{M}$  and  $\bar{K}$ , as well as the half-zone point between  $\bar{\Gamma}$  and  $\bar{M}$ , we distort the equilibrium geometry according to the two-dimensional wave vector under consideration. We then calculate the intraplanar and interplanar force constants coupling the outermost layer to the interior layers from first principles. The surface force constants are then used together with bulk force constants obtained from neutron scattering experiments [17] to set up a dynamical matrix for a fifty-layer slab. By diagonalizing this matrix, eigenvalues and eigenvectors for the bulk and surface modes are obtained. Examining the surface intralayer force constants we found a small softening of  $\sim 8\%$  for Ag(111) and  $\sim 13\%$  for Cu(111). It is worth mentioning that this approach goes beyond the conventional "frozen phonon" calculation because no assumptions about the eigenvectors have to be made. In Table I, we show a comparison between experiment, taken from Ref. [2], and theory for the low-lying Rayleigh mode  $S_1$  at the high symmetry points  $\bar{M}$  and  $\bar{K}$ . The agreement with experiment is excellent.

To resolve the z-polarized and longitudinal localized structures, it is best to carry out a systematic comparison between theory and experiment of the EELS cross section at different impact energies and scattering geometries. The three panels of Fig. 2 illustrate this procedure. For the calculations, the eigenvectors and eigenvalues of the first-principles calculations are fed into a multiple-scattering slab calculation to evaluate the EELS cross section. Comparisons with experimental data taken from Ref. [7] are made at  $\bar{M}$  for Cu(111) at the following scattering conditions: (a)  $E_i = 110$  eV,  $\theta_i = 78.3^\circ$ ; (b)  $E_i = 175$  eV,  $\theta_i = 49.1^\circ$ ; and (c)  $E_i = 150$  eV,  $\theta_i = 48.1^\circ$ , respectively. These scattering conditions are chosen because at condition (a), the Rayleigh mode  $S_1$  is the strongest and the data show a sharp peak at  $107 \text{ cm}^{-1}$

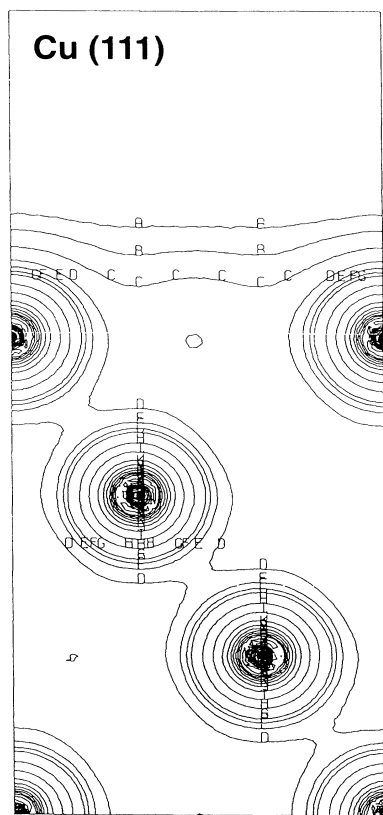


FIG. 1. Contours of constant charge density for Cu(111) in the  $(\bar{1}10)$  plane.

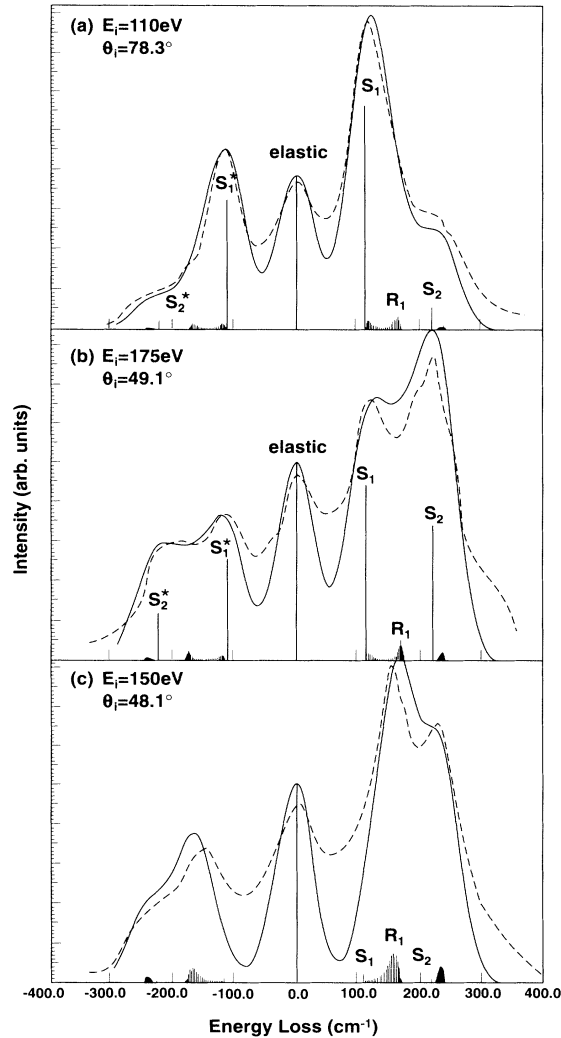


FIG. 2. Calculated (solid line) and measured (dashed line) electron-energy-loss spectra for Cu(111) at  $\bar{M}$ . Each vertical line represents an individual mode energy-loss intensity. The elastic intensity is fitted to data, taken from Ref. [7]. The calculated curves are obtained by Gaussian broadening the individual energy-loss intensities with a full width at half maximum of  $55 \text{ cm}^{-1}$ . The asterisk denotes energy-gain cross section.

with a weak shoulder above  $200 \text{ cm}^{-1}$ . The two features correspond well to the loss cross sections of  $S_1$  and  $S_2$ , respectively. The  $z$ -polarized resonance provides  $R_1$  little contribution to the EELS spectra under condition (a). Under condition (b), while the contribution from  $R_1$  remains small, the relative intensities between the  $S_1$  and  $S_2$  modes are reversed. Here, the  $S_2$  mode dominates over the spectra. Finally, under condition (c), the cross sections of both  $S_1$  and  $S_2$  are small, while that of the resonance  $R_1$  is large. Therefore, the nature of the multimode contributions to the EELS spectra is unravelled in these comparisons. The EELS spectra are consistent with the results of three surface localized modes along  $\bar{\Gamma}\bar{M}$ :

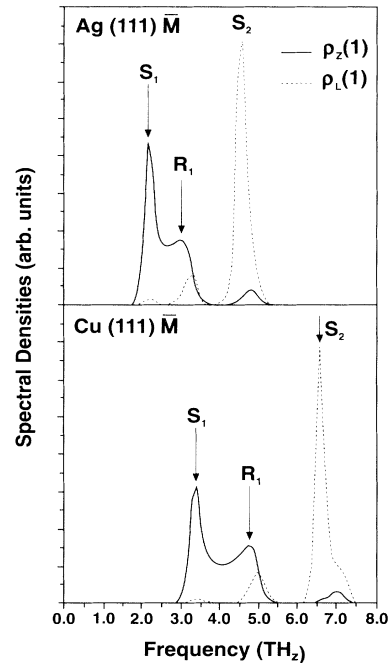


FIG. 3. Calculated phonon spectral densities at  $\bar{M}$  in Cu(111) and Ag(111) using the first-principles method.  $\rho_z(1)$  is the surface-layer shear vertical component and  $\rho_L(1)$  is the surface-layer longitudinal component. The measured frequencies by HAS and EELS are indicated by arrows.

$S_1$  (Rayleigh),  $R_1$  ( $z$ -polarized resonance), and  $S_2$  (longitudinal gap mode). In Figs. 2(a)-2(c), there is also a contribution from a resonance near the top of the bulk phonon band. This resonance has a small first-layer  $z$  polarization and a large second-layer longitudinal polarization.

In Fig. 3, the surface layer phonon spectral densities at  $\bar{M}$  are shown for Cu(111) and Ag(111). In both cases, the spectral densities show two surface modes  $S_1$  and  $S_2$  and a  $z$ -polarized resonance  $R_1$ . The arrows indicate peak positions from either HAS or EELS measurements; specifically,  $S_1$  and  $R_1$  for Ag(111) and Cu(111) were first measured by HAS [1,2] while  $S_2$  for Cu(111) was measured by EELS [7]. Along the  $\bar{\Gamma}\bar{K}$  direction, the situation is more complicated due to the fact that there is no mirror plane, thus resulting in a mixture of shear horizontal and sagittal plane modes. Our first-principles results again show three localized modes: The lowest two branches are  $z$  polarized while the highest branch is longitudinal. These results again explain well the existing HAS data [1,2]. It is also interesting to point out that the first-principles results along the  $\bar{\Gamma}\bar{K}$  direction are in agreement with those obtained by the EAM model [8]. Both sets of theoretical calculations along  $\bar{\Gamma}\bar{K}$  predict three localized structures: The  $z$ -polarized  $S_1$  (Rayleigh wave), a higher  $z$ -polarized pseudo-Rayleigh wave (PRW), and a longitudinal mode. We present in Figs.

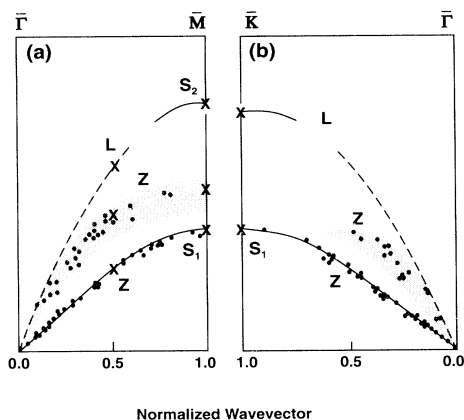


FIG. 4. Schematic surface phonon dispersions along  $\bar{\Gamma}\bar{M}$  and  $\bar{\Gamma}\bar{K}$  for Ag(111). Only even-symmetry components are shown with shear vertical ( $z$ ) and longitudinal ( $L$ ) polarizations. Crosses mark first-principles calculated frequencies and dots denote HAS data.

4(a) and 4(b) the localized structures along  $\bar{\Gamma}\bar{M}$  and  $\bar{\Gamma}\bar{K}$  for Ag(111) determined by first-principles theory (crosses) along with HAS data [2] (dots).

In summary, results of first-principles calculations together with cross-section calculations of EELS rule out large softening in the intralayer surface force constants or the presence of anomalous longitudinal resonances on these surfaces as proposed in previous studies. It is clear from Figs. 4(a) and 4(b) that the longitudinal modes (dashed lines) are substantially higher in frequency than those of the HAS (dots) measurement. Instead, we explain the higher mode measured by HAS along  $\bar{\Gamma}\bar{M}$  as due to a  $z$ -polarized  $R_1$  resonance. This mode seems to be absent in all the previous parameter-based phonon calculations. Along  $\bar{\Gamma}\bar{K}$ , the first-principles studies support again the  $z$  polarization for the two modes measured by HAS, a result consistent with the findings of EAM [8]. The combination of first-principles lattice dynamics with multiple-scattering EELS cross-section calculations was previously used to clarify the number of modes and their polarizations on Cu(001) and Ag(001) [18]. Results of these studies suggest that highly accurate theoretical models are necessary for the proper characterization of surface lattice dynamics on even simple metallic surfaces.

This work is supported by DOE Grant No. DE-FG0284ER45076. Work at Ames Laboratory is supported by DOE Contract No. W-7405-Eng-82. K.P.B., T.R.,

and K.M.H. acknowledge the support of NATO Grant No. RG(8610516).

- [1] R. B. Doak, U. Harten, and J. P. Toennies, *Phys. Rev. Lett.* **51**, 578 (1983).
- [2] U. Harten, J. P. Toennies, and Ch. Wöll, *Faraday Discuss. Chem. Soc.* **80**, 137 (1985).
- [3] V. Bortolani, A. Franchini, F. Nizzoli, and G. Santoro, *Phys. Rev. Lett.* **52**, 429 (1984).
- [4] V. Bortolani, G. Santoro, U. Harten, and J. P. Toennies, *Surf. Sci.* **148**, 82 (1984); V. Bortolani, A. Franchini, F. Nizzoli, and G. Santoro, *ibid.* **152/153**, 811 (1985).
- [5] C. S. Jayanthi, H. Bilz, W. Kress, and G. Benedek, *Phys. Rev. Lett.* **59**, 795 (1987).
- [6] V. Bortolani, F. Ercolessi, E. Tosatti, A. Franchini, and G. Santoro, *Europhys. Lett.* **12**, 149 (1990).
- [7] M. H. Mohamed, L. L. Kesmodel, B. M. Hall, and D. L. Mills, *Phys. Rev. B* **37**, 2763 (1988); B. M. Hall, D. L. Mills, M. H. Mohamed, and L. L. Kesmodel, *ibid.* **38**, 5856 (1988).
- [8] J. S. Nelson, M. S. Daw, and E. C. Sowa, *Phys. Rev. B* **40**, 1465 (1989).
- [9] S. A. Lindgren, L. Wolldin, J. Rundgren, and P. Westrin, *Phys. Rev. B* **29**, 576 (1984).
- [10] K. P. Bohnen, Th. Rodach, and K. M. Ho, in *Structure of Surface-III*, edited by S. Y. Tong, M. A. Van Hove, K. Takayanagi, and X. D. Xie (Springer, Berlin, 1991).
- [11] V. Bortolani, A. Franchini, and G. Santoro (unpublished).
- [12] See, for example, K. M. Ho and K. P. Bohnen, *J. Electron Spectrosc. Relat. Phenom.* **54/55**, 229 (1990).
- [13] D. R. Hamann, M. Schlüter, and C. Chiang, *Phys. Rev. Lett.* **43**, 1494 (1979).
- [14] L. Hedin and B. I. Lundqvist, *J. Phys. C* **4**, 2064 (1971).
- [15] H. Hellmann, *Einführung in die Quantenchemie* (Deuticke, Leipzig, 1937); R. P. Feynman, *Phys. Rev.* **56**, 340 (1939).
- [16] The calculated relaxations in terms of percentage of the bulk interlayer spacing are  $\Delta d_{12} = -1.3$ ,  $\Delta d_{23} = -0.6$  and  $\Delta d_{12} = -0.4$ ,  $\Delta d_{23} = -0.2$  for Cu(111) and Ag(111), respectively. Low-energy diffraction determination of  $\Delta d_{12} = -0.7$  for Cu(111) is given by Ref. [9].
- [17] *Metals: Phonon States and Electron States and Fermi Surfaces*, edited by K. H. Hallwege and J. L. Olsen, Landolt-Börnstein, New Series, Group 3, Vol. 13 (Springer, New York, 1981).
- [18] Y. Chen, S. Y. Tong, M. Rocca, P. Moretto, U. Valbusa, K. P. Bohnen, and K. M. Ho, *Surf. Sci. Lett.* **250**, L389 (1991); Y. Chen, S. Y. Tong, J. S. Kim, L. L. Kesmodel, T. Rodach, K. P. Bohnen, and K. M. Ho, *Phys. Rev. B* **44**, 11394 (1991).